THE JOURNAL OF PHYSICAL CHEMISTRY B

Article

pubs.acs.org/JPCB

Peptides with the Same Composition, Hydrophobicity, and Hydrophobic Moment Bind to Phospholipid Bilayers with Different Affinities

Melissa A. Cherry, Sarah K. Higgins, Hilary Melroy, Hee-Seung Lee, and Antje Pokorny*

Department of Chemistry and Biochemistry, University of North Carolina Wilmington, Wilmington, North Carolina 28403, United States

ABSTRACT: We investigated the dependence of membrane binding on amino acid sequence for a series of amphipathic peptides derived from δ-lysin. δ-Lysin is a 26 amino acid, N-terminally formylated, hemolytic peptide that forms an amphipathic α-helix bound at membrane−water interfaces. A shortened peptide, lysette, was derived from δ-lysin by deletion of the four N-terminal amino acid residues. Five variants of lysette were synthesized by altering the amino acid sequence such that the overall hydrophobic moment remained essentially the same for all peptides. Peptide−lipid equilibrium dissociation constants and helicities of peptides bound to zwitterionic lipid vesicles were determined by stopped-flow fluorescence and circular dichroism. We found that binding to phosphatidylcholine bilayers was a function of the helicity of the bound peptide alone and independent of the *a priori* hydrophobic moment or the ability to form intramolecular salt bridges. Molecular dynamics (MD) simulations on two of the peptides suggest that sequence determines the insertion depth into the bilayer. The location of the two aspartate residues at the C-terminus of lysette-2 leads to a loss of helical content in the simulations, which correlates with faster desorption from the bilayer as compared to lysette. We also found a systematic deviation of the experimentally determined dissociation constant and that predicted by the Wimley−White interfacial hydrophobicity scale. The reason for the discrepancy remains unresolved but appears to correlate with a predominance of isoleucine over leucine residues in the lysette family of peptides.

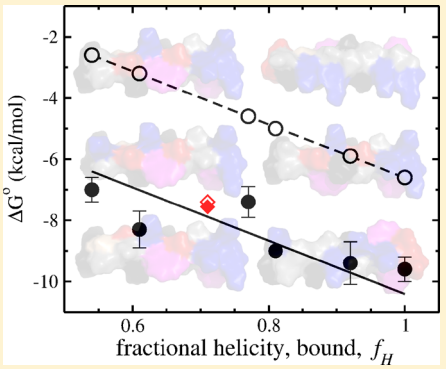

INTRODUCTION

The interaction of α-helical amphipathic peptides with phospholipid bilayers and the resulting disturbance of membrane integrity, however transient, forms the basis of a number of important biological phenomena, including the action of many antimicrobial peptides. These tend to be cationic peptides, between 15 and 35 amino acids long, that interact preferentially with the anionic cell membranes of bacteria and fungi. In general, specificity for a certain type of membrane correlates with peptide hydrophobicity and charge.[1−4] Amino acid sequence plays a role in the sense that shuffling the sequence of any peptide often abolishes peptide activity *in vivo* but sometimes leads to variants that are equally or even more active.[5] Yet, sequence shuffling also impacts hydrophobic moment and helix propensity, which complicates the correlation of experiment with a unique structural feature of the peptide. To address the importance of amino acid sequence in a more quantitative way, we designed a series of sequence variants of the synthetic peptide lysette. Lysette is a shortened version of staphylococcal δ-lysin that lacks the four N-terminal amino acids of the full-length peptide. Lysette and δ-lysin interact strongly with lipid bilayer vesicles composed of zwitterionic phosphatidylcholine (PC) and cause rapid release of their content. In contrast to the full-length peptide, which has no net charge at pH 7, lysette and its sequence variants carry a net charge of +2 at neutral pH, which makes them better mimics of antimicrobial peptides. Moreover, the increased charge reduces peptide aggregation in solution relative to the parent peptide, δ-lysin. The lysette sequence variants were designed under the constraint that the hydrophobic moment be essentially the same for all peptides. Overall charge and hydrophobicity are also preserved among the variants, since they contain the same amino acids. Some of the peptide sequences are almost entirely scrambled with respect to the original lysette, while in others about 90% of the original sequence is conserved. Any differences in peptide binding can then be correlated with sequence features and their influence on peptide−membrane interactions assessed.

The experimentally determined Wimley−White (WW) interfacial hydrophobicity scale provides a convenient and generally accurate method of estimating the Gibbs free energy of α-helical peptide binding to neutral phospholipid bilayers.[6−8] The scale was established by determining the partitioning of a series of pentapeptides between an aqueous phase and POPC bilayers through equilibrium dialysis. The pentapeptides contained a central residue to be tested, flanked Leu and Trp

Received: July 21, 2014
Revised: October 6, 2014
Published: October 20, 2014

residues to ensure peptide location at the bilayer−water interface. The WW interfacial scale obtained in this fashion was later successfully used to characterize the membrane−water partitioning of a family of six 17-residue peptides, the AQL peptides.[36,38] The method is based on the idea that the Gibbs free energy of binding of the entire peptide, ΔG°, is the sum of the individual contributions from each amino acid, plus a term that accounts for backbone hydrogen bond formation resulting from helix formation at the interface. The formation of backbone hydrogen bonds that accompanies helix formation contributes ≈−0.4 kcal/mol/residue to ΔG°.[9,10] The WW interfacial scale is one of a number of hydrophobicity scales that have been used to predict the partitioning of amino acid residues and peptides into lipid bilayers.[6,11−17] All existing hydrophobicity scales are correlated to a large degree, although the magnitudes of the determined Gibbs free energies of interaction differ.[18] Among the published hydrophobicity scales, the WW interfacial scale is particularly useful because it is a whole residue, not only a side chain scale. Moreover, the pentapeptides used to establish the scale were designed to ensure the confinement of the residue of interest to the bilayer−water interface.

The degree to which polar and nonpolar residues are segregated along the helix axis is given by the hydrophobic moment, μ_H, which is the mean vector sum of the hydrophobicities, H_i, of the amino acid side chains in a helical peptide, $\langle\mu_H\rangle = \sum_{i=1}^{N}\vec{H}_i/N$, where N is the number of residues.[19] The hydrophobic moment is often thought to be a good predictor for the helicity of the bound peptide, but we show here that this is clearly not the case.

We found that in spite of all peptides being characterized by approximately the same hydrophobic moment in an all-helical conformation, the sequence variants were helical to different degrees when bound to 1-palmitoyl-2-oleoyl- *sn*-glycero-3-phosphocholine (POPC) bilayers, indicating that the *a priori* hydrophobic moment is a poor predictor of peptide binding. However, the helicity of the bound peptide was found to clearly correlate with the dissociation constant, K_D, and the Gibbs free energy of binding determined experimentally, ΔG°_{exp}. We also found that ΔG°_{exp} was independent of the inferred ability to form intermolecular salt bridges. To better understand the experimental results, we performed molecular dynamics (MD) simulations on two of the peptides bound to a POPC bilayer. The MD simulations suggest that the peptide location at the membrane−water interface is affected by the distribution of cationic and anionic residues along the sequence and their interactions with the lipid headgroups. Binding of all lysette variants to vesicles composed of POPC depended strongly on the amino acid sequence and was significantly and systematically more favorable than predicted from the Wimley−White interfacial hydrophobicity scale, ΔG°_{WW}. The origin of the discrepancy between the calculated and measured values of ΔG° remains unclear but appears to correlate with a high abundance of Ile in the nonpolar faces of peptides that belong to the lysette family.

METHODS

Chemicals. 1-Palmitoyl-2-oleoyl-*sn*-glycero-3-phosphocholine (POPC) was purchased from Avanti Polar Lipids (Alabaster, AL). Carboxyfluorescein (99% pure, lot A015252901) was purchased from ACROS (Morris Plains, NJ). 1-Palmitoyl-2-oleoyl-*sn*-glycero-3-phosphoethanolamine-*N*-(7-methoxycoumarin) (7MC-POPE), POPE labeled with 7MC through an amide bond to the amino group of the ethanolamine headgroup, was synthesized in our lab as previously described.[20] Organic solvents (HPLC/ACS grade) were purchased from Burdick & Jackson (Muskegon, MI). Lipids and probes were tested by TLC and used without further purification. All peptides were custom synthesizd by New England Peptide LLC (Gardner, MA) at 95% purity. Stock peptide solutions were prepared by dissolving lyophilized peptide in distilled water at a final concentration of about 200 μM and stored at −80 °C. The peptide concentration of the stock solution was determined precisely by measuring the absorbance at 280 nm and using a molar extinction coefficient of tryptophan of 5600 M^{-1} cm^{-1}.

Preparation of Large Unilamellar Vesicles. Large unilamellar vesicles (LUVs) were prepared by mixing the lipids in chloroform in a round-bottom flask. For vesicles containing 7MC-POPE, the probes were added to the lipid in chloroform solution at a final probe concentration of 2 mol %. The solvent was rapidly evaporated using a rotary evaporator (Büchi R-3000, Flawil, Switzerland) at 60 °C. The lipid film was then placed under vacuum for 4 h and hydrated by the addition of buffer containing 20 mM MOPS, pH 7.5, 0.1 mM EGTA, 0.02% NaN_3, and 100 mM KCl or 10 mM phosphate buffer. The suspension of multilamellar vesicles was subjected to five freeze−thaw cycles and extruded 10× through two stacked polycarbonate filters of 0.1 μm pore size (Nuclepore, Whatman, Florham, NJ), in a water-jacketed high pressure extruder (Lipex Biomembranes, Inc., Vancouver, Canada) at room temperature. Lipid concentrations were assayed by the Bartlett phosphate method,[21] modified as previously described.[22]

Kinetics of Peptide Binding to and Dissociation from Lipid Vesicles. The kinetics of association of the lysette peptides with LUVs were recorded on an Applied Photophysics SX.18 MV stopped-flow fluorometer (Leatherhead, Surrey, UK). Fluorescence resonance energy transfer (FRET) between the Trp residue intrinsic to all lysette peptides and 7MC-POPE incorporated in the lipid membrane was used to monitor peptide binding and dissociation from LUVs. The Trp was excited at 280 nm and transferred energy to 7MC-POPE, which absorbs maximally at 348 nm. The emission of 7MC, with a maximum at 396 nm, was measured using a GG-385 high pass filter (Edmund Industrial Optics, Barrington, NJ). After mixing, the concentration of peptide was 0.5 μM.

CD Spectroscopy. CD spectra of all peptide variants in solution and bound to POPC vesicles were obtained on a Chirascan CD spectrometer (Applied Photophysics, Leatherhead, Surrey, UK) in a 0.1 cm path length quartz cuvette (Starna Cells Inc., Atascadero, CA). All CD spectra were taken in 10 mM phosphate buffer, pH 7.5. CD spectra of peptides bound to POPC LUVs were taken at a peptide concentration of 20 μM and a lipid concentration of 5 mM to ensure complete peptide binding. The use of concentrated LUV suspensions in CD measurements has been discussed in detail and shown to yield accurate results.[23] A lipid baseline spectrum was subtracted from all peptide spectra and the resulting trace smoothed in Chirascan Pro-Data, maintaining random residuals. Fractional helicities were determined according to Luo and Baldwin.[24] The fractional helicity (f_H) of a peptide is

$$f_H = \frac{\Theta_{obs} - \Theta_C}{\Theta_H - \Theta_C} \quad (1)$$

where Θ_{obs} is the measured helicity. The helicity of the random coil (Θ_C) was set to 1500, and Θ_H, the helicity of the complete helix, was calculated according to

$$\Theta_H(T) = \left[\Theta_H(0) + T\frac{d\Theta_H}{dT}\right](1 - x/N_{res}) \quad (2)$$

The number of residues is given by N_{res}, T is the temperature in °C, x = 2.5, and $\Theta_H(0)$ = −44 000.[24]

Wimley−White Interfacial Scale. The free energies of peptide binding from water to the membrane water interface according to the Wimley−White interfacial scale, ΔG°_{WW}, were calculated using the totalizer routine available in the online tool Membrane Protein Explorer, Mpex.[25,26] For each peptide sequence, the values listed in Table 2 were obtained choosing the interface scale (IF), assuming free end groups (protonated N-terminus and deprotonated C-terminus), and the experimentally determined helicities of the lipid-bound peptides.

Molecular Dynamics Simulation. All molecular dynamics simulations were performed using the GROMACS 4.0 package.[27] Starting configurations consisted of 128 POPC molecules[28] and a helical peptide placed in one of two locations with respect to the bilayer. For the first set of simulations the peptide was placed 15−20 Å above the bilayer surface. Simulation time for these sets was 400 ns. In the second set, the peptide was placed in the interfacial region, just below the lipid head groups. Simulation time for the interfacial simulations was 200 ns. All simulations were carried out with a periodic boundary condition at constant temperature (323 K) and pressure (1 atm). To maintain the temperature, the Nosé−Hoover thermostat was employed, and pressure was maintained with the Parrinello−Rahmann barostat. The peptide was described by the ffgmx force field supplied with the GROMACS 4.0 package and the lipids by the Berger force field.[29] The particle-mesh-Ewald (PME) was used to define electrostatic interaction with a real-space cutoff of 1.0 nm. The van der Waals cutoff was also set at 1.0 nm. All simulations used a time step of 2 fs. In order to maintain a neutral environment, Cl^- counterions were added to each system. Each simulation began with a short energy minimization step to remove any nonphysical interaction, followed by a 1−2 ns long position restrained run to ensure the water molecules were settled around the peptide−membrane system. The subsequence production runs were carried out under NPT condition without any constraint. Helicities of the final structures were analyzed using the software DSSP.[30]

RESULTS

Peptide Design. The lysette peptide variants designed for this study are based on an N-terminally truncated version of the naturally occurring peptide δ-lysin. Their sequences (Table 1) are such that the hydrophobic moment of the all-helical conformation is conserved throughout the family as seen from the helical wheel projections in Figure 1A and Table 2. As a result, roughly the same residues occupy the polar and nonpolar peptide faces in most lysettes (Figure 1B). A single Trp residue occupies a central position in the polar face of lysette. That position is maintained in lysette-K and lysette-28 but has been exchanged for a Leu residue in lysette-26. In lysette-24, the Trp residue has been moved to the nonpolar face, along with the two Asp residues that are now located at the N-terminus (Figure 1).

Table 1. Amino Acid Sequences for Lysette and the Five Sequence Variants[a]

peptide	sequence
lysette	IISTIGDLVKWIIDTVNKFTKK
lysette-K	IIKTIGDLVKWIIDTVNSFTKK
lysette-28	IIGTIDSLVKWIIDTVNKFTKK
lysette-24	DDNVIGKIWSKLITVITKIFTK
lysette-26	IISTIGDWVKLIIDTVNKFTKK
lysette-2	LIKNIGTIVSKIIKTVWKFTDD

[a]N- and C-termini are unmodified.

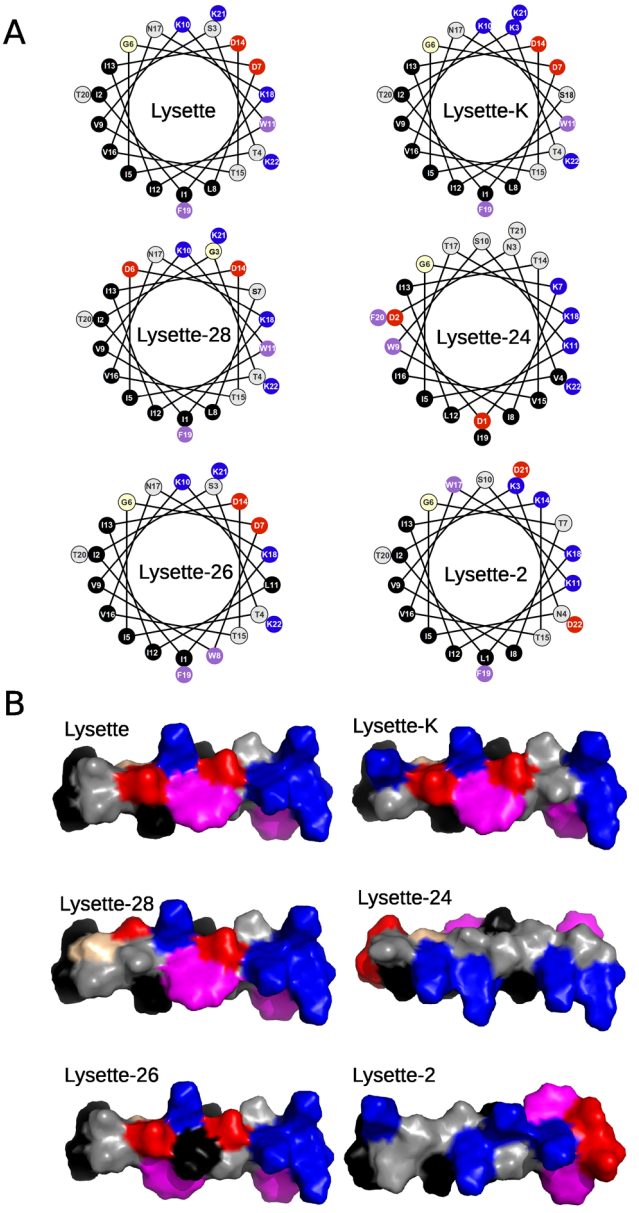

Figure 1. Peptide structures in all-helical conformations. (A) Helical wheel projections of all peptides studied. (B) α-Helical surface plots, viewed from the polar face. Lys residues are shown in blue, Asp in red, aromatic amino acids in magenta, and Gly in light brown. All other polar side chains are shown in light gray and nonpolar residues in black.

Peptide Binding. Peptide binding to unilamellar POPC vesicles was measured by the increase in FRET from the

intrinsic Trp residue of the peptides to a fluorescent lipid probe incorporated in the membrane. A kinetic trace showing the fluorescence increase of the acceptor fluorophore 7MC-POPE following peptide binding is shown in Figure 2A, and the

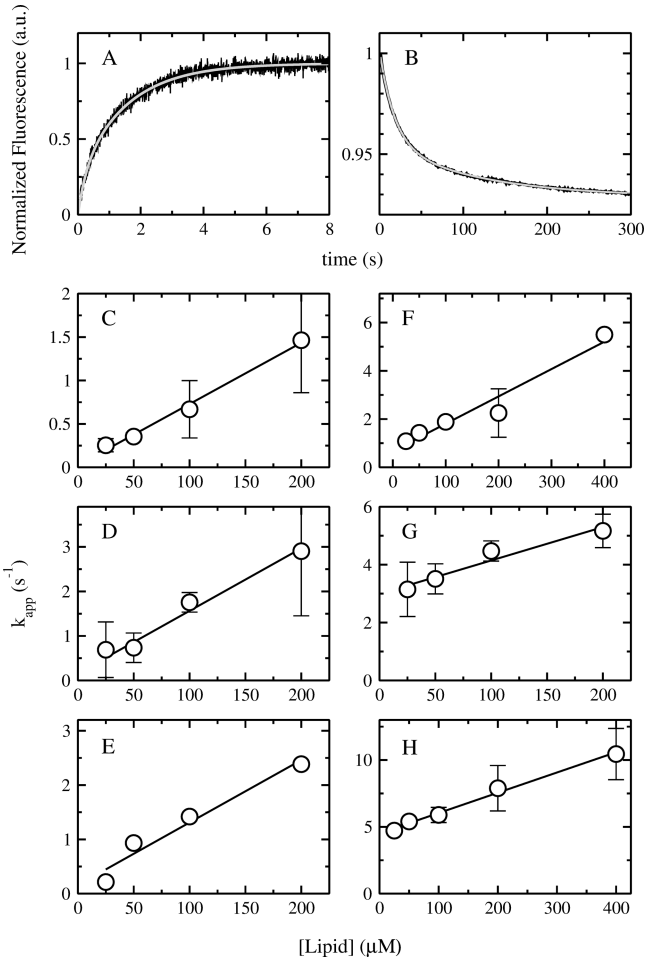

Figure 2. Kinetics of peptide binding to POPC bilayers and determination of on and off rate constants. (A) Association of lysette (0.5 μM) with POPC vesicles (100 μM), measured by FRET. The smooth line is a two-exponential fit to the experimental data. (B) Kinetics of peptide desorption from POPC vesicles. Peptide (lysette, 1 μM) was premixed with 150 μM POPC LUV containing 7MC-POPE and allowed to bind. This suspension was then mixed with POPC acceptor vesicles (final POPC concentration was 475 μM) in a stopped-flow mixer. The smooth line is a two-exponential fit to the experimental data. The major phase corresponds to peptide desorption from the vesicles. (C–H) k_{app} for all peptides as a function of lipid concentration, empty symbols. With the exception of (E), all data points are averages from a minimum of two independent data sets. A linear regression to the experimental data yields k_{on} from the slope and k_{off} from the y-intercept.

complete kinetic analysis of binding curves as a function of lipid concentration is summarized in Figure 2C–H. The molecular rate constants for peptide binding, k_{on}, and desorption, k_{off}, are obtained from the slope and y-intercept of the linear regressions shown in Figure 2C–H.[31,32] In cases where k_{off} is very small, the error in the determination from the linear regressions can be large. Therefore, we also determined k_{off} in a separate experiment, in which the peptides are first incubated with vesicles containing the acceptor fluorophore 7MC-POPE. In a second step, these vesicles are mixed with an excess of unlabeled vesicles. The peptides will re-equilibrate over the entire vesicle population at a rate that is limited by the rate constant of peptide desorption from the donor vesicles, k_{off} (Figure 2B). The dissociation constant is given by $K_D = k_{off}/k_{on}$. To be able to relate the experimentally determined K_D to the Wimley–White hydrophobicity scale, K_D must be converted to a partition coefficient in units of mole fraction, which is achieved by dividing K_D by the concentration of water, [W] = 55.5 M.[6,7] The Gibbs free energies of binding to POPC vesicles are then obtained from the relationship $\Delta G^{\circ}_{exp} = RT \ln K_D - \ln[W]$. The molecular rate constants, K_D, and ΔG°_{exp} are listed in Table 2.

CD Spectroscopy. We determined the helicity of all peptides at low concentration (2 μM) in buffer (Figure 3A) and bound to POPC vesicles (Figure 3B) from the ellipticity at 222 nm.

The change in helicity that occurs upon peptide binding is an important parameter in the determination of ΔG°_{WW} because the formation of an α-helix at the bilayer–water interface contributes a favorable free energy of about −0.4 kcal/mol/residue to the Gibbs free energy of binding as a result of hydrogen bond formation between amide groups in the peptide backbone.[9,10] All lysettes form helices when bound to the membrane but to different degrees (Figure 3B). With the exception of lysette-2, the peptides show some degree of helicity in buffer (Figure 3A), which suggests that, in aqueous solution, either the peptide monomers are partially helical or some oligomers coexist with monomers. The AGADIR algorithm[33,34] predicts random coil structures for all monomeric lysette peptides in solution, making the latter possibility the more likely. In the calculation of ΔG°_{WW}, however, we assumed that binding occurs from an unstructured peptide in solution to a final folded state at the membrane–water interface. This assumption seems justified because in a recent detailed study of the kinetics of interaction of lysette-26 with POPC bilayers we showed that of the species present in solution, only the peptide monomers, but not the oligomers, bind to the bilayer in the time frame of the experiment.[31] The experimentally determined dissociation constants, the Gibbs free energies of binding, ΔG°_{exp}, derived from K_D, and the helicities of the membrane-bound states are tabulated in Table 2, along with Gibbs free energy of binding derived from the Wimley–White interfacial scale, ΔG°_{WW}.

MD Simulations. We performed MD simulations of lysette and lysette-2 interacting with a POPC bilayer. The two peptides only share 50% sequence identity and are at the opposite end of K_D and helicity scales shown in Table 2. Of all peptides studied here, lysette-2 shows the weakest binding and lowest degree of helicity.

The simulations were started with the peptides already in a helical conformation since they are not expected to form helices from a random coil structure within the time scale of MD simulation. In the simulations shown in Figure 4A–F, the peptides were oriented with the hydrophobic peptide face pointing toward the bilayer. Simulations in which the peptides had the opposite orientation did not show significantly different final results. With this starting configuration, both lysette and lysette-2 rotate by roughly 90°as the peptides approach the bilayer, placing the polar side closer to the bilayer (when the simulations were started with the opposite orientation, the peptides did not reorient). In all simulations, the peptides eventually become parallel to the bilayer after making full contact with the lipid head groups. After this initial contact, the

dx.doi.org/10.1021/jp507289w | J. Phys. Chem. B 2014, 118, 12462–12470

Table 2. Hydrophobic Moments (μ_H), Molecular Rate Constants of Binding (k_{on}) and Dissociation (k_{off}), Dissociation Constants (K_D), Fractional Helicities of the Membrane-Bound Peptides (f_H), and Values for the Gibbs Free Energy of Binding Determined Experimentally (ΔG°_{exp}) and from the Wimley–White Interfacial Scale (ΔG°_{WW}) for All Lysette Peptides[a]

peptide	μ_H	k_{on} (M^{-1} s^{-1})	k_{off} (s^{-1})	K_D (μM)	ΔG°_{exp} (kcal/mol)	f_H	ΔG°_{WW} (kcal/mol)	$\Delta\Delta G^\circ_{exp-WW}$[b] (kcal/mol)
lysette	6.67	7.1×10^3	0.033	4.6	−9.6 ± 0.4	1	−6.6	−3.0
lysette-K	7.09	1.4×10^4	0.11	7.5	−9.4 ± 0.7	0.92	−5.9	−3.5
lysette-28	6.43	1.2×10^4	0.17	15	−9.0 ± 0.1	0.81	−5.0	−4.0
lysette-24	7.92	1.1×10^4	0.48	42	−8.3 ± 0.6	0.61	−3.2	−5.1
lysette-26	6.67	1.2×10^4	2.2	190	−7.4 ± 0.5	0.77	−4.6	−2.8
lysette-2	6.67	1.5×10^4	6.1	400	−7.0 ± 0.4	0.55	−2.6	−4.4

[a]The differences between ΔG°_{exp} and ΔG°_{WW} ($\Delta\Delta G^\circ_{exp-WW}$) are listed in the last column. The error in k_{on} (fit error) is on the order of 20%, that in k_{off} (SD) ≈ 40%, and that in K_D (SD) ≈ 50%. The error in f_H (SD) does not exceed 10%. [b]Calculated using the program MPEx[25,26] and the experimentally determined f_H.

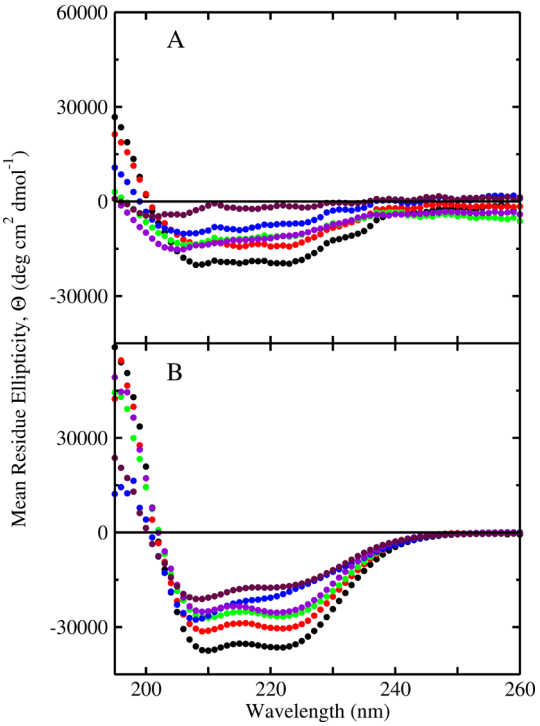

Figure 3. CD spectra of peptides in solution and bound to POPC LUVs. (A) Peptides in buffer at a concentration of 2 μM. (B) Peptides (20 μM) bound to POPC LUVs. Lipid concentration was 5 mM to ensure complete binding. Lysette, black; lysette-K, red; lysette-28, green; lysette-24, blue; lysette-26, magenta; lysette-2, brown. Helicities of the bound states are listed in Table 2.

peptides pivot around their long axis, insert more deeply into the bilayer core, and now orient their nonpolar faces toward the bilayer interior, while maintaining contact with the polar lipid headgroups. Figure 4A,B shows the location of the center-of-mass of each peptide with respect to the bilayer center as a function of simulation time. For comparison, the time evolution of the center-of-mass of the phosphorus and ester oxygen atoms at the lipid tails is also shown. Clearly, lysette-2 is able to penetrate more deeply into the bilayer than lysette by the end of the simulation, whereas lysette barely passes the phosphorus atoms after 400 ns of simulation time. Snapshots at the end of 400 ns simulation time are shown in Figure 4E,F.

The difference in peptide sequence between lysette and lysette-2 appears to influence the insertion depth of the charged residues, Lys and Asp. Figure 4C,D shows the time evolution of the center-of-mass for the side chain of each charged residue. The location of the two anionic Asp residues appears to have a large impact on the final peptide location. In lysette-2, the two Asp residues are located at the C-terminus, whereas they occupy more central positions in lysette. Throughout the simulation, their terminal location in lysette-2 allows the Asp residues to remain above the bilayer and exposed to water. By contrast, in the lysette simulation, the Asp side chains are forced into the bilayer and are located close to the choline head groups by the end of the simulation.

The Lys residues are spread throughout the sequence in both peptides, but only the insertion of lysette-2 is accompanied by "snorkeling" of the Lys residues: the long Lys methylene side chains are mostly located below the ester oxygens from where they reach toward the hydrophilic headgroup, allowing the terminal amino group to form a salt bridge with a lipid phosphate group (Figure 4F,H). Salt-bridge formation probably hinders further peptide insertion, and we expect the peptide to remain below the ester oxygen with its hydrophobic side facing the bilayer core. We observed similar behavior in MD simulations of transportan-10 (TP10) interacting with a POPC bilayer.[35] By contrast, in the lysette simulations, the Lys side chains are mostly found around or above the ester oxygen (Figure 4C) with the terminal amino group in the Lys residues maintaining salt bridges to the lipid phosphates. Intramolecular salt bridges between Lys and Asp can potentially form in lysette between residues 7 and 10, 10 and 14, 14 and 18 and at the C-terminus. However, intramolcular salt bridges were found to rarely form and be very short-lived in comparison to those formed between Lys and the lipid phosphate groups.

After 400 ns simulation time, lysette appears less helical at the interface than lysette-2 (Figure 4E,F), which is not supported by the experimental data (Figure 3). This strongly suggests that the peptide structures adopted after 400 ns of simulation time are not equilibrium structures. To access more representative structures without unreasonably extending the simulation time, we performed two additional simulations, in which the peptides were placed directly into the bilayer interface (Figure 4G,H). After 200 ns, the centrally located Asp residues in lysette prevent the peptide from inserting beyond the lipid carbonyl groups, but the peptide is largely helical. In the lysette-2 interface simulation, the Lys residues maintain contact with the lipid phosphate groups, while the majority of the peptide is located below the lipid carbonyl groups. The centers-of-mass of the C-terminal Asp residues remain above the lipid phosphates, as seen previously, forcing the peptide to lose helical content at the C-terminus. While it is difficult to quantitatively compare experimental helicities with those

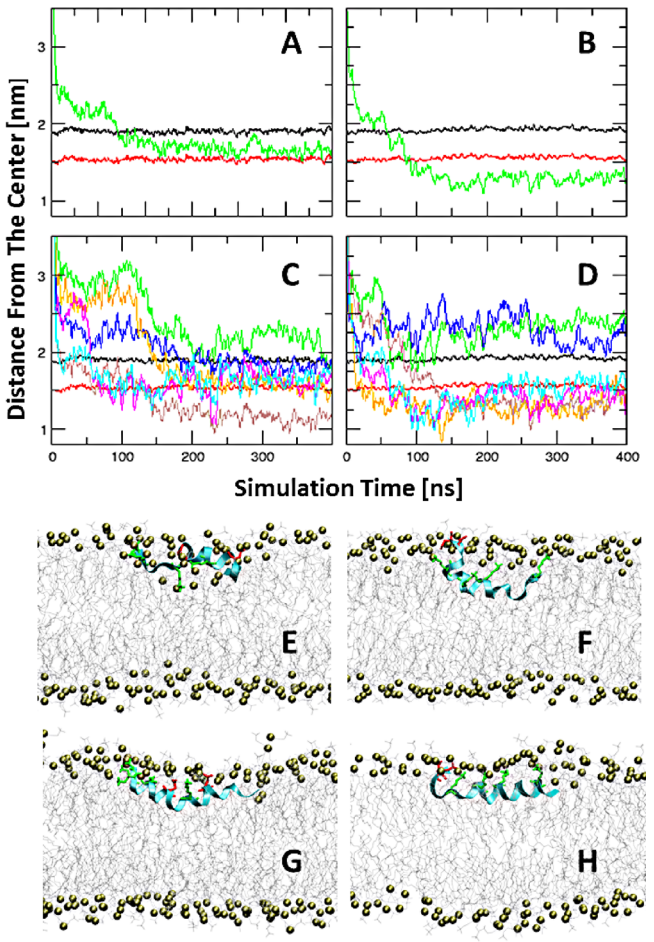

Figure 4. Time evolution of the peptide center-of-mass distances and of all charged residues and snapshots of peptide configurations for the lysette (left-hand panels) and lysette-2 simulations (right-hand panels) bound to a POPC bilayer. (A) Center-of-mass distance from the bilayer center for lysette as a function of simulation time (green). For reference, the center-of-mass distances of the phosphorus (black) and ester oxygen atoms (red) are also included. (B) Center-of-mass distance from the bilayer center for lysette-2 as a function of simulation time (green). (C) Lysette, time evolution of the center-of-mass of the charged residues Lys and Asp from the bilayer center. The center-of-mass distances of the phosphorus (black) and ester oxygen atoms (red) are included. (D) Lysette-2, time evolution of the enter-of-mass of the charged residues Lys and Asp from the bilayer center. Color schemes in (C) and (D) are as follows: green, D7; blue, D14; orange, K10; brown, K18; magenta, K21; and cyan, K22 for the lysette simulation, and green, D21; blue, D22; orange, K3; brown, K11; magenta, K14; and cyan, K18 for the lysette-2 simulation. (E) Snapshot of the lysette simulation after 400 ns. Asp side chains, red, and Lys side chains, green. (F) Snapshot of the lysette-2 simulation after 400 ns. Asp side chains, red, and Lys side chains, green. (G) Snapshot of the lysette interface simulation after 200 ns. Asp side chains, red, and Lys side chains, green. (H) Snapshot of the lysette-2 interface simulation after 200 ns. Asp side chains, red, and Lys side chains, green.

obtained from MD simulations, lysette is significantly more helical at the end of the interface simulation than lysette-2 (73%, compared with 64% for lysette-2).

DISCUSSION

We measured binding of a series of closely related peptides derived from δ-lysin to lipid bilayers composed of POPC. The peptide variants studied differ in amino acid sequence but not in composition and have very similar hydrophobic moments in all-helical conformations. We compared the experimentally determined dissociation constants with those predicted by the WW interfacial scale, which is, in general, an excellent predictor of α-helical peptide binding to neutral lipid bilayers.[36−38] The data allow four main conclusions to be drawn.

First, we found that ΔG° of binding correlates with the helicity of the bound state (Table 2). Indeed, the plot in Figure 5A (solid symbols) shows that ΔG°_{exp} is a linear function of the

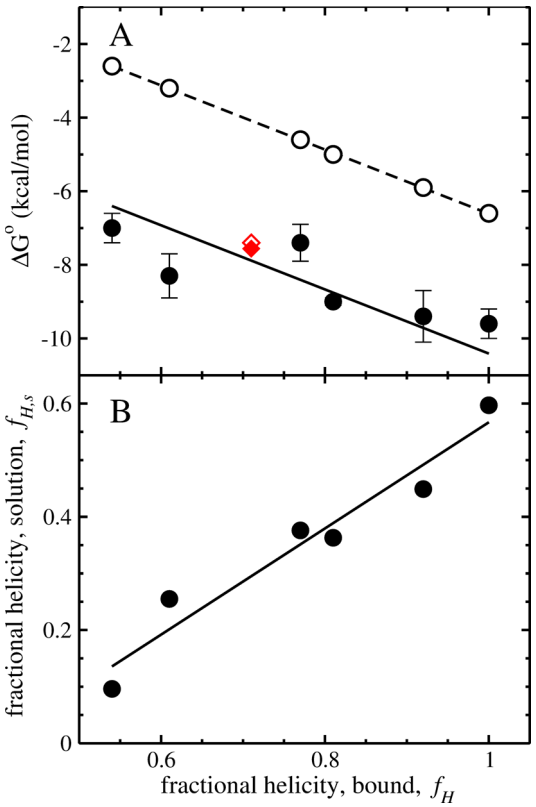

Figure 5. Gibbs free energy of binding, ΔG°, and degree of helicity in solution as a function of fractional helicity of the bound state, f_H, for the lysette family of peptides and melittin. (A) ΔG° as a function of fractional helicity bound to the lipid bilayer. Lysette family, black symbols, and melittin, red symbols. ΔG°_{WW}, empty symbols. The dashed line is a linear regression to the data points obtained for the lysette peptides. ΔG°_{exp}, solid symbols. The slope of the solid line is the same as that of the dashed line to indicate the systematic discrepancy between ΔG°_{exp} and ΔG°_{WW}. (B) Fractional helicities for all lysette peptides in solution, $f_{H,s}$, plotted as a function of the fractional helicity of the bound state.

helicity of the membrane-bound state. Moreover, ΔG°_{exp} exhibits the same dependence on fractional helicity as ΔG° calculated from the WW interfacial hydrophobicity scale (open symbols), using the experimentally determined helicities of the membrane-bound peptides. Since all lysette peptides have approximately the same calculated hydrophobic moment, ΔG° is shown to be independent of the hydrophobic moment of the all-helical conformation. In other words, the *a priori* hydrophobic moment, μ_H, of the peptide helix is a poor predictor of the degree of helicity of the bound state. It is simply a measure of the degree of the segregation of polar and nonpolar amino acids along the peptide axis, indicative of the potential of the peptide helix to form. To what degree the helix actually forms is

dx.doi.org/10.1021/jp507289w | J. Phys. Chem. B 2014, 118, 12462−12470

determined by helix-stabilizing side chain interactions, which depend on sequence. Thus, actual helix propensities can vary widely among peptides of the same composition, if residues are shuffled only within a peptide face such that μ_H is maintained. The helicity of the bound peptide also correlates linearly with the peptide helicity in solution, $f_{H,s}$ (Figure 5B), as has previously been observed for the synthetic AQL peptide series.[36]

We conclude that for peptides of identical composition binding to neutral bilayers is a function only of the degree of helicity of the bound state. Weak binding of peptides with low helicity is due to the energetically unfavorable transfer of unsatisfied hydrogen bonds in the nonhelical peptide backbone to the membrane−water interface. Membrane binding is, thus, not a function of the amphipathicity of the peptide helix, a conclusion that is further supported by the observation that synthetic α/β-peptides possess strong antibacterial activity despite their inability to form an amphipathic structure.[39] Rather, it is the sequence that directly determines the degree of helicity of the membrane-bound state and, therefore, its binding affinity. Since the helicity of the peptide in solution and bound to the membrane correlate with ΔG° of binding, an accurate theoretical prediction of peptide helicities in aqueous solution would, in principle, allow the prediction of peptide affinity for neutral bilayers from first principles.

Closer inspection of Table 2 indicates that all sequence changes introduced relative to the original lysette destabilize the lipid-bound helices, leading to faster desorption from the bilayer surface (larger k_{off} in Table 2 and Figure 2). Lysette and lysette-2 occupy the two extremes in Table 2, with lysette-2 showing the weakest binding of the peptides studied here. One of the most obvious differences between lysette and lysette-2 is the distribution of the two Asp residues, which are located within the sequence, at positions 7 and 14, in lysette but at the C-terminus in lysette-2. The C-terminal location of the Asp residues in lysette-2 has some important consequences. For one, it allows the Asp residues to remain in or even above the polar headgroup region and exposed to bulk water, thus minimizing the energetically unfavorable transfer of Asp residues to the membrane−water interface.[6,17] This also allows the remainder of the peptide to sink into the bilayer hydrophobic core, while the centrally located Lys residues remain in contact with the lipid phosphate groups (Figure 4). However, the favorable location of Asp above the lipid phosphates comes at the cost of unraveling the peptide helix at the C-terminus (Figure 4F,H), which is a known consequence of C-terminal Asp residues.[40,41] The MD simulations thus corroborate the experimental observation that the helicity of lipid-bound lysette-2 is low relative to other peptides in the series (Table 2 and Figure 4G,H), promoting fast desorption from the bilayer. By contrast, the center-of-mass of lysette remains above the lipid phosphate region, and the centrally located Asp residues are pulled further into the lipid headgroup region by the end of the simulation, which allows the peptide to remain largely helical.

Second, we can exclude the possibility that peptide intramolecular salt bridges contribute significantly to ΔG°_{exp}. We had originally hypothesized that intramolecular salt bridges would contribute to a more favorable ΔG° because the transfer of oppositely charged ion pairs to the membrane−water interface should be more favorable than that of isolated, charged side chains.[42] However, the arrangement of residues in two of the studied peptides, lysette-24 and lysette-2, prohibits extensive salt-bridge formation (Table 1), but K_D still scales with helicity of the bound species, just as for all the other peptides in the series (Figure 5). This result is supported by the MD simulations, which did not find stable intramolecular salt bridges between Lys and Asp in Lysette (data not shown). The conclusion that intramolecular salt bridges do not play a significant role in peptide binding to lipid bilayers was also reached in the case of DL-1, a variant of full-length δ-lysin, in which all Asp residues had been replaced by Lys[43] and for a series of peptides unrelated to those investigated here.[37,43]

Third, a favorable contribution to the Gibbs free energy of binding due to snorkeling of Lys residues, which is absent from the WW interfacial scale,[44] is unlikely to play a role in the binding of the lysette family of peptides. In our MD simulations, significant Lys snorkeling is only observed for lysette-2, not lysette, yet the ΔG°_{exp} is a linear function of the degree of helicity of the bound state (Figure 5).

Fourth, we found a systematic discrepancy between the experimental Gibbs free energies of binding (ΔG°_{exp}) and those predicted by the WW interfacial scale (ΔG°_{WW}) on the order of −4 kcal/mol for the entire family of lysette peptides. The experimentally determined Gibbs free energies of binding and those predicted by the WW scale show the same linear dependence on helicity (Figure 5A), which simply reflects the −0.4 kcal/mol/residue of the free energy originating from the formation of a backbone hydrogen bond at the interface. However, the ΔG°_{exp} plot (solid symbols) is shifted on the ordinate with respect to ΔG°_{WW} (open symbols) by −4 kcal/mol (Figure 5A). Since this is true for all the lysette peptides irrespective of sequence, it appears that, in the main, only the types of residues are responsible for the shifted ΔG°_{exp} values, but not their specific order.

Could different methods used in the determination of ΔG° account for the observed discrepancy? The WW scale has been established using equilibrium dialysis, whereas we have determined ΔG° through the analysis of kinetic binding data. For many peptides, however, the determination of K_D and thus ΔG° from kinetic binding data is well established, $K_D = k_{off}/k_{on}$.[4,32,37] Nonetheless, we verified that the method gives the same results as equilibrium measurements for one of the most studied peptide, melittin. To this end, we determined binding of melittin to POPC LUVs through $K_D = k_{off}/k_{on}$. The results compare extremely well with those obtained by the equilibrium dialysis method (Figure 5, red symbols). Thus, differences in methodology cannot account for the observed discrepancy. We have already excluded peptide intramolecular salt bridges as a significant contribution to ΔG°. Additional interactions between residue side chains in the folded state, such as hydrogen bonds and cation−π interactions,[45−47] can also contribute to a more favorable ΔG° by reducing the free energy cost of transferring charged or polar groups from water to the bilayer−water interface.[42] However, all specific side chain interactions require a precise positioning of the residues involved in forming the interaction and can thus not be responsible for the observed effect.

If the experimental data are reliable, could the WW interfacial scale itself be the source of the discrepancy? The WW scale has been shown in many cases to be a reliable predictor of peptide binding at membrane interfaces. Thus, its failure to correctly predict the binding of the lysette family of peptides is more likely to reside with a feature of this particular set of peptides. What, then, distinguishes the lysette peptide series and other peptides that show better than predicted binding to POPC

bilayers from those whose binding agrees with the WW scale? An interesting pattern emerges when comparing the compositions of the lysette family and the antimicrobial peptide cecropin A with those of melittin, TP10W, and the AQL family of peptides. Cecropin A, just like the lysettes, binds better than predicted to POPC vesicles by −4.7 kcal/mol,[43] whereas melittin, TP10W, and the AQL peptides fit the WW interfacial scale very well.[36,37] The nonpolar faces of the lysettes and cecropin A contain Ile in preference over Leu; however, in melittin, TP10W, and the AQL peptides Ile occurs less frequently or not at all, and Leu is more abundant.

Our current results are consistent with the idea that membrane binding of peptides with a preponderance of Leu residues over Ile is well described by the WW interfacial scale, whereas the opposite is true for peptides with a high Ile content relative to Leu. This suggests that either the WW interfacial scale is incorrect for Ile or that, in the peptides studied here, Ile is not located at the membrane−water interface, but perhaps closer to the membrane core. If Ile were more deeply inserted into the bilayer, its partitioning into the bilayer should be more appropriately described by the WW octanol scale, with octanol mimicking the hydrocarbon interior of the bilayer. The WW octanol scale lists −1.12 kcal/mol for the Gibbs free energy of partitioning from water to octanol for Ile.[14] Using this value, ΔG°_{WW} for the lysettes and cecropin A becomes more favorable by −4 kcal/mol, which agrees with our experimentally determined values.

Two related questions arise: what is special about Ile over Leu and the other hydrophobic residues? And, if the peptides indeed insert more deeply, would Leu not also be exposed to the hydrocarbon interior and experience a different Gibbs free energy of partitioning? First, Ile and Leu are much more common in membrane-binding peptides than other hydrophobic residues and will thus determine to a large extent peptide hydrophobicity. Second, Ile and Leu partition similarly into the bilayer−water interface and octanol, according to the WW scales.[14] However, MD simulations suggest that Ile and Leu may actually behave quite differently in a lipid bilayer. Calculations of the potentials of mean force (PMF) that amino acid residues experience as they are moved along the bilayer normal show a more favorable PMF for Ile than Leu in both the lipid headgroup region and the bilayer interior,[17] which was attributed to a better packing of the Ile side chain in the bilayer than that of Leu.

AUTHOR INFORMATION

Corresponding Author

*Tel (910) 962-4231; Fax (910) 962-3013; e-mail almeidaa@uncw.edu (A.P.).

Notes

The authors declare no competing financial interest.

ACKNOWLEDGMENTS

This work was supported by National Institutes of Health Grants AI088567 and GM072507. We thank Paulo Almeida for many helpful discussions.

REFERENCES

(1) Tossi, A.; Sandri, L.; Giangaspero, A. Amphipathic, alpha-helical antimicrobial peptides. *Biopolymers* **2000**, *55*, 430.

(2) Zasloff, M. Antimicrobial peptides of multicellular organisms. *Nature* **2002**, *415*, 389−395.

(3) Tachi, T.; Epand, R. F.; Epand, R. M.; Matsuzaki, K. Position-dependent hydrophobicity of the antimicrobial magainin peptide affects the mode of peptide-lipid interactions and selective toxicity. *Biochemistry* **2002**, *41*, 10723−10731.

(4) Almeida, P. F.; Pokorny, A. Interactions of Antimicrobial Peptides with Lipid Bilayers. In *Comprehensive Biophysics*; Tamm, L., Egelman, E. H., Eds.; Academic Press: Oxford, 2012; Vol. *5*, pp 189−222.

(5) Hilpert, K.; Elliott, M. R.; Volkmer-Engert, R.; Henklein, P.; Donini, O.; Zhou, Q.; Winkler, D. F.; Hancock, R. E. Sequence requirements and an optimization strategy for short antimicrobial peptides. *Chem. Biol.* **2006**, *10*, 1101−1107.

(6) Wimley, W. C.; White, S. H. Experimentally determined hydrophobicity scale of proteins at membrane interfaces. *Nat. Struct. Biol.* **1996**, *3*, 842848.

(7) White, S. H.; Wimley, W. C. Membrane protein folding and stability: Physical principles. *Annu. Rev. Biophys. Biomol. Struct.* **1999**, *28*, 319365.

(8) Hristova, K.; White, S. H. An experiment-based algorithm for predicting the partitioning of unfolded peptides into phosphatidylcholine bilayer interfaces. *Biochemistry* **2005**, *44*, 1261412619.

(9) Ladokhin, A. S.; White, S. H. Folding of amphipathic alpha-helices on membranes: Energetics of helix formation by melittin. *J. Mol. Biol.* **1999**, *285*, 13631369.

(10) Almeida, P. F.; Pokorny, A. Mechanisms of antimicrobial, cytolytic, and cell-penetrating peptides: from kinetics to thermodynamics. *Biochemistry* **2009**, *48*, 80838093.

(11) MacCallum, J. L.; Bennett, W. F.; Tieleman, D. P. Partitioning of amino acid side chains into lipid bilayers: results from computer simulations and comparison to experiment. *J. Gen. Physiol.* **2007**, *129*, 371−377.

(12) Wolfenden, R. Experimental measures of amino acid hydrophobicity and the topology of transmembrane and globular proteins. *J. Gen. Physiol.* **2007**, *129*, 357−362.

(13) Wimley, W. C.; Creamer, T. P.; White, S. H. Solvation energies of amino acid side chains and backbone in a family of host-guest pentapeptides. *Biochemistry* **1996**, *35*, 5109−5124.

(14) Wimley, W. C.; White, S. H. Hydrophobic interactions of peptides with membrane interfaces. *Biochim. Biophys. Acta* **1998**, *1376*, 339−352.

(15) Moon, C. P.; Fleming, K. G. Side-chain hydrophobicity scale derived from transmembrane protein folding into lipid bilayers. *Proc. Natl. Acad. Sci. U. S. A.* **2011**, *108*, 10174−10177.

(16) Hessa, T.; Meindl-Beinker, N. M.; Bernsel, A.; Kim, H.; Sato, Y.; Lerch-Bader, M.; Nilsson, I.; White, S. H.; von Heijne, G. Molecular code for transmembrane-helix recognition by the Sec61 translocon. *Nature* **2007**, *450*, 1026−1030.

(17) MacCallum, J. L.; Bennett, W. F.; Tieleman, D. P. Distribution of amino acids in a lipid bilayer from computer simulations. *Biophys. J.* **2008**, *94*, 3393−3404.

(18) MacCallum, J. L.; Tieleman, D. P. Hydrophobicity scales: a thermodynamic looking glass into lipid-protein interactions. *Trends Biochem. Sci.* **2011**, *36*, 653−662.

(19) Eisenberg, D.; Weiss, R. M.; Terwilliger, T. C. The helical hydrophobic moment: a measure of the amphiphilicity of a helix. *Nature* **1982**, *299*, 371−374.

(20) Gregory, S. M.; Cavenaugh, A. C.; Journigan, V.; Pokorny, A.; Almeida, P. F. F. A quantitative model for the all-or-none permeabilization of phospholipid vesicles by the antimicrobial peptide cecropin A. *Biophys. J.* **2008**, *94*, 16671680.

(21) Bartlett, G. R. Phosphorous assay in column chromatography. *J. Biol. Chem.* **1959**, *234*, 466468.

(22) Pokorny, A.; Birkbeck, T. H.; Almeida, P. F. F. Mechanism and kinetics of delta-lysin interaction with phospholipid vesicles. *Biochemistry* **2002**, *41*, 1104411056.

(23) Ladokhin, A. S.; Fernandez-Vidal, M.; White, S. H. CD spectroscopy of peptides and proteins bound to large unilamellar vesicles. *J. Membr. Biol.* **2010**, *236*, 247253.

(24) Luo, P.; Baldwin, R. L. Mechanism of helix induction by trifluoroethanol: A framwork for extrapolating the helix- forming properties of peptides from trifluoroethanol/water mixtures back to water. *Biochemistry* **1997**, *36*, 84138421.
(25) Snider, C.; Jayasinghe, S.; Hristova, K.; White, S. H. MPEx: a tool for exploring membrane proteins. *Protein Sci.* **2009**, *18*, 2624−2628.
(26) MPEx, the membrane protein explorer, is available online at http://blanco.biomol.uci.edu/mpex/.
(27) Hess, B.; Kutzner, C.; van der Spoel, D.; Lindahl, E. GROMACS 4: Algorithms for highly efficient, load-balanced, and scalable molecular simulation. *J. Chem. Theory Comput.* **2008**, *4*, 435−447.
(28) Tieleman, D. P.; Forrest, L. R.; Sansom, M. S.; Berendsen, H. J. Lipid properties and the orientation of aromatic residues in OmpF, influenza M2, and alamethicin systems: molecular dynamics simulations. *Biophys. J.* **1998**, *37*, 17554−17561.
(29) Berger, O.; Edholm, O.; Jahnig, F. Molecular dynamics simulations of a fluid bilayer of dipalmitoylphosphatidylcholine at full hydration, constant pressure, and constant temperature. *Biophys. J.* **1997**, *72*, 2002−2013.
(30) Kabsch, W.; Sander, C. Dictionary of protein secondary structure: pattern recognition of hydrogen-bonded and geometrical features. *Biopolymers* **1983**, *22*, 2577−2637.
(31) Kreutzberger, A. J.; Pokorny, A. On the origin of multiphasic kinetics in peptide binding to phospholipid vesicles. *J. Phys. Chem. B* **2012**, *116*, 951957.
(32) Almeida, P. F.; Pokorny, A. Binding and permeabilization of model membranes by amphipathic peptides. In *Methods in Molecular Biology*; Giuliani, A., Rinaldi, A. C., Eds.; Humana Press: New York, 2010; Vol. *618*, pp 155−169.
(33) Muñoz, V.; Serrano, L. Development of the multiple sequence approximation within the Agadir model of -helix formation. Comparison with Zimm-Bragg and Lifson-Roig formalisms. *Biopolymers* **1997**, *41*, 495509.
(34) AGADIR, an algorithm to predict the helical content of peptides, is available on-line at http://agadir.crg.es/.
(35) Dunkin, C. M.; Pokorny, A.; Almeida, P. F.; Lee, H. S. Molecular dynamics studies of transportan 10 (TP10) interacting with a POPC lipid bilayer. *J. Phys. Chem. B* **2011**, *115*, 1188−1198.
(36) Fernández-Vidal, M.; Jayasinghe, S.; Ladokhin, A. S.; White, S. H. Folding amphipathic helices into membranes: amphiphilicity trumps hydrophobicity. *J. Mol. Biol.* **2007**, *370*, 459−470.
(37) McKeown, A. N.; Naro, J. L.; Huskins, L. J.; Almeida, P. F. A thermodynamic approach to the mechanism of cell-penetrating peptides in model membranes. *Biochemistry* **2012**, *50*, 654−662.
(38) Almeida, P. F.; Ladokhin, A. S.; White, S. H. Hydrogen-bond energetics drive helix formation in membrane interfaces. *Biochim. Biophys. Acta* **2012**, *1818*, 178−182.
(39) Schmitt, M. A.; Weisblum, B.; Gellman, S. H. Interplay among folding, sequence, and lipophilicity in the antibacterial and hemolytic activities of alpha/beta-peptides. *J. Am. Chem. Soc.* **2006**, *129*, 417−428.
(40) Huyghues-Despointes, B. M.; Scholtz, J. M.; Baldwin, R. L. Effect of a single aspartate on helix stability at different positions in a neutral alanine-based peptide. *Protein Sci.* **1993**, *2*, 16041611.
(41) Doig, A. J.; Baldwin, R. L. N- and C-capping preferences for all 20 amino acids in alpha-helical peptides. *Protein Sci.* **1995**, *4*, 1325−1336.
(42) Wimley, W. C.; Gawrisch, K.; Creamer, T. P.; White, S. H. Direct measurement of salt-bridge solvation energies using a peptide model system: Implications for protein stability. *Proc. Natl. Acad. Sci. U. S. A.* **1996**, *93*, 29852990.
(43) Clark, K. S.; Svetlovics, J.; McKeown, A. N.; Huskins, L.; Almeida, P. F. What determines the activity of antimicrobial and cytolytic peptides in model membranes. *Biochemistry* **2011**, *50*, 7919−7932.
(44) Aliste, M. P.; Tieleman, D. P. Computer simulation of partitioning of ten pentapeptides Ace-WLXLL at the cyclohexane/water and phospholipid/water interfaces. *BMC Biochem.* **2005**, *6*, 30.
(45) Marqusee, S.; Baldwin, R. L. Helix stabilization by Glu^{-}...Lys^{+} salt bridges in short peptides of de novo design. *Proc. Natl. Acad. Sci. U. S. A.* **1987**, *84*, 8898−8902.
(46) Huyghues-Despointes, B. M.; Klingler, T. M.; Baldwin, R. L. Measuring the strength of side-chain hydrogen bonds in peptide helices: the Gln.Asp (i, i + 4) interaction. *Biochemistry* **1995**, *34*, 13267−13271.
(47) Luo, P.; Baldwin, R. L. Origin of the different strengths of the (i,i+4) and (i,i+3) leucine pair interactions in helices. *Biophys. Chem.* **2002**, *96*, 103−108.